Switching Speedup of the Magnetic Free Layer of Advanced SOT-MRAM

Roberto L. de Orio[1], Alexander Makarov[2], Siegfried Selberherr[2], Wolfgang Goes[3], Johannes Ender[1], Simone Fiorentini[1], and Viktor Sverdlov[1]
[1]*Christian Doppler Laboratory for Nonvolatile Magnetoresistive Memory and Logic at the*
[2]*Institute for Microelectronics, TU Wien, Austria*
[3]*Silvaco Europe Ltd., Cambridge, United Kingdom*
{orio|sverdlov}@iue.tuwien.ac.at

***Abstract*—We investigate the switching of a symmetric square and an elongated rectangular perpendicular free layer by spin-orbit torque with a magnetic field-free two-pulse scheme. The switching of the layer is achieved by utilizing the in-plane shape anisotropic magnetic field. For making the switching of a symmetric square layer deterministic, an in-plane stray field created in a part of the layer is used. The combination of the shape and stray fields accelerates the switching of the free layer significantly. A switching speedup factor of 3 to 5 has been obtained. The strategy also improves the robustness of the scheme allowing fast, sub-0.5 ns switching, less sensitive to the pulses' properties.**

***Index Terms*—Spin-Orbit MRAM, perpendicular magnetization, magnetic field-free switching, two-pulse switching scheme**

I. Introduction

Spin-transfer torque magnetic RAM (STT-MRAM) is fast, possesses high endurance (10^{12}), and has a simple structure. It is compatible with CMOS technology and can be straightforwardly embedded in circuits [1]. It is particularly promising for use in IoT and automotive applications, as a replacement of conventional flash memory, as well as for embedded applications [2].

Although the use of STT-MRAM in last-level caches is possible [3], the switching current for operating at a speed faster than 10 ns is fairly high. The large current densities flowing through magnetic tunnel junctions lead to oxide reliability issues which in turn reduce the MRAM endurance. Thus, devices based on a new principle are required.

Spin-orbit torque (SOT) assisted switching of a free layer (FL) is promising, because it combines non-volatility, high-speed, and high-endurance [4]. In this memory cell the magnetic tunnel junction's (MTJ) free layer is grown on a material with a large spin Hall angle. The relatively large switching current is passing through a heavy normal metal (NM) wire on which the FL is grown [5]. The write current does not flow through the MTJ, while a much smaller read current is applied through the MTJ. This results in a three-terminal configuration where the read and write current paths are decoupled. Since the large write current does not flow through the oxide in the MTJ, this prevents the tunnel barrier from damage and improves device reliability. However, a static magnetic field is still required for deterministic switching [6] of the FL. Even though several paths to achieve a field-free switching were reported [7], [8], [9], these require a local intrusion into the cell fabrication, which makes large scale integration problematic.

In this work we demonstrate that the switching of a symmetric square layer can be made deterministic by creating an in-plane stray field in a part of the FL. The switching of the rectangular perpendicular magnetized FL is accomplished by the in-plane shape anisotropic magnetic field. The combination of the shape and stray fields accelerates the switching of the FL significantly. Our results indicate a switching speedup factor of 3 to 5. Moreover, it improves the robustness of scheme allowing fast, sub-0.5 ns switching.

II. Device Structures and Modeling

The structure of the symmetric square and the rectangular device are shown in Fig. 1. Both structures consist of a perpendicularly magnetized FL grown on top of a heavy metal

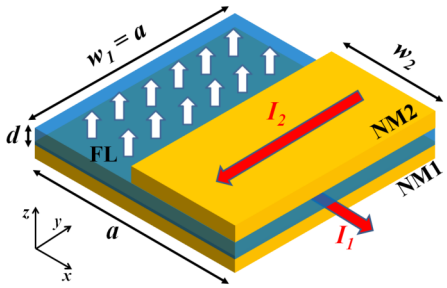

(a)

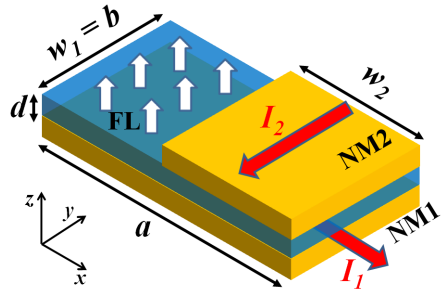

(b)

Fig. 1: Two-pulse switching scheme applied to the perpendicularly polarized square magnetic FL. (a) Symmetric square FL. (b) Rectangular FL.

TABLE I: Parameters used in the simulations [10].

Saturation magnetization, M_S	1×10^6 A/m
Exchange constant, A	1×10^{-11} J/m
Effective Perpendicular anisotropy, K	4.2×10^5 J/m^3
Gilbert damping, α	0.02
Spin Hall angle, θ_{SH}	0.3
Free layer dimensions (square)	15×15×2 nm^3
Free layer dimensions (rectangular)	25×10×2 nm^3

wire (NM1) of $l = 3$ nm thickness. Another heavy metal wire (NM2) also of $l = 3$ nm thickness lies on top of the FL. The parameters of the FL are listed in Table I.

The dimensions of the the square structure are $a \times a \times d = 15 \times 15 \times 2\,\text{nm}^3$, while the rectangular device has $a \times b \times d = 25 \times 10 \times 2\,\text{nm}^3$, where a represents the length, b represents the width, and d is the thickness of the FL. These dimensions guarantee a thermal stability factor of about 50. As Fig. 1 shows, the FL fully overlaps with the NM1. Thus, the NM1 width is $w_1 = 15$ nm for the symmetric and $w_1 = 10$ nm for the non-symmetric device. In order to investigate the effect of the stray field acting on part of the FL, NM2 wires of different widths, w_2, have been considered. For the symmetric square $w_2 = a = 15$ nm and $w_2 = 10$ nm are used. For the non-symmetric rectangular device $w_2 = b = 25$ nm and $w_2 = 10$ nm are simulated.

The magnetic field-free switching of the devices is based on a two-current pulse scheme previously proposed in [11]. This scheme works as following: First, a pulse of a fixed duration $T_1 = 100$ ps and fixed current density $j_1 = 12 \times 10^{12}$ A/m^2, "Pulse 1", is applied through the NM1. The critical current density for switching the device is about 10^{13} A/m^2. Then, a second consecutive perpendicular pulse, "Pulse 2", is applied through the NM2. This pulse provides the same current density as the first pulse. However, "Pulse 2" has a variable duration T_2 in order to investigate the effect of different pulse configurations on the switching dynamics of the device.

The magnetization dynamics of the magnetic system is described by the Landau-Lifshitz-Gilbert equation supplemented with the SOT generated by the current pulses acting on the FL, which can be written as

$$\begin{aligned}\frac{\partial \mathbf{m}}{\partial t} &= -\gamma \mathbf{m} \times \mathbf{H_{eff}} + \alpha \mathbf{m} \times \frac{\partial \mathbf{m}}{\partial t} \\ &+ \gamma \frac{\hbar}{2e} \frac{\theta_{SH} j_1}{M_S d} \left[\mathbf{m} \times (\mathbf{m} \times \mathbf{y})\right] \Theta(t)\Theta(T_1 - t) \\ &- \gamma \frac{\hbar}{2e} \frac{\theta_{SH} j_2}{M_S d} \left[\mathbf{m} \times (\mathbf{m} \times \mathbf{x})\right] \Theta(t - T_1)\Theta(T_2 + T_1 - t),\end{aligned} \tag{1}$$

where $\mathbf{m}$ is the position-dependent magnetization $\mathbf{M}$ normalized by the saturation magnetization M_S, γ is the gyromagnetic ratio, α is the Gilbert damping, and $\mathbf{H_{eff}}$ is an effective magnetic field, e is the elementary charge, $\hbar$ is the Plank constant, and θ_{SH} is an effective Hall angle. The effective field $\mathbf{H_{eff}}$ includes the exchange, uniaxial perpendicular anisotropy, demagnetization, and random thermal field at 300 K. To describe the magnetization dynamics, we employ our in-house open-source tool [12] based on the finite difference discretization method. The parameters used in the simulations are given in Table I.

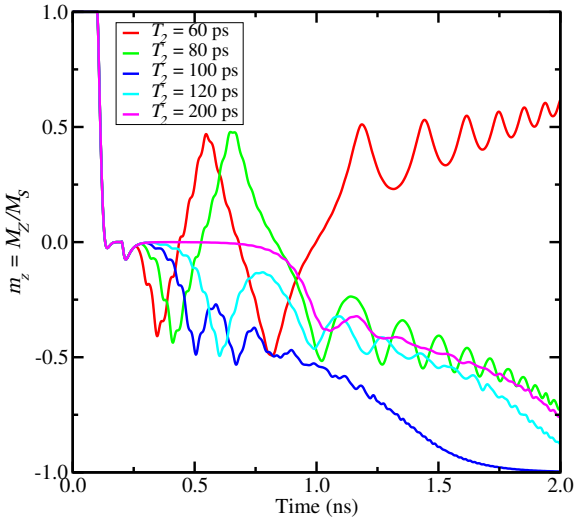

Fig. 2: Average magnetization (z component) for several pulses durations T_2 for the rectangular device.

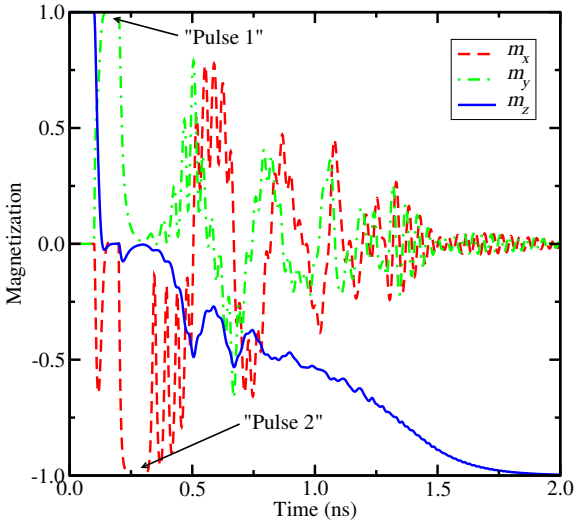

Fig. 3: Components of the magnetization vector for the rectangular device and $T_2 = 100$ ps. The first pulse puts the magnetization in y direction on the FL plane and the second pulse pushes the magnetization to $-x$ direction.

III. Results

Considering, initially, the rectangular structure with $w_2 = 25$ nm, the FL is fully covered by the layer NM2, Fig. 2 shows the z component of the magnetization vector as a function of time for different durations of "Pulse 2" (T_2). The magnetization is taken as the average out of 20 different realizations (due to the random thermal field) for the same current pulse configurations. Deterministic switching (i.e. all realizations lead to switching) of the free layer is observed for $T_2 \geq 80$ ps.

The dynamics of the magnetization components is shown in Fig. 3 for $T_2 = 80\,\text{ps}$. When "Pulse 1" is turned on, the magnetization is placed on the plane of the FL along the y direction ($m_z = 0$, $m_y = +1$) as the first torque term in (1) suggests. This condition is explicitly depicted as "Pulse 1" in Fig. 3. Then, the magnetization under the layer NM2 gets rotated towards $-x$ direction ($m_x = -1$, "Pulse 2" in Fig. 3) due to the SOT of the second pulse, corresponding to the second torque term in (1). At this point, the shape anisotropy plays an important role as an effective magnetic field which pushes the magnetization towards switching. The switching process is further supported by the uniaxial perpendicular anisotropy of the FL.

Considering now the symmetric square structure with $w_2 = a = 15\,\text{nm}$, Fig. 4 shows the magnetization of several realizations. Here, the switching is not deterministic, i. e., part of the realizations switch, part of the realizations do not. No "Pulse 2" parameters were detected which would support deterministic switching of the FL.

This is in contrast to the SOT-MRAM cell with the rectangular FL layer, where the shape anisotropy plays the role of the effective magnetic field, while the switching direction is determined by the polarity of "Pulse 2" which pushes the magnetization to one or another side from the in-plane direction along the short side of the rectangle [11]. As there is no shape anisotropy for a square, i.e a symmetric FL, the switching is unreliable, as observed in Fig. 4.

In order to break the symmetry of the square structure, the width of the layer NM2 is reduced, so that the square FL is only partially covered. The resulting magnetization dynamics for $w_2 = 10\,\text{nm}$ is shown in Fig. 5. Reliable switching is observed for all values of T_2. Moreover, the switching time is significantly reduced. For instance, for $T_2 = 100\,\text{ps}$, the switching time of the rectangular structure is 0.9 ns, while for the square FL with non-symmetric NM2 it is 0.5 ns.

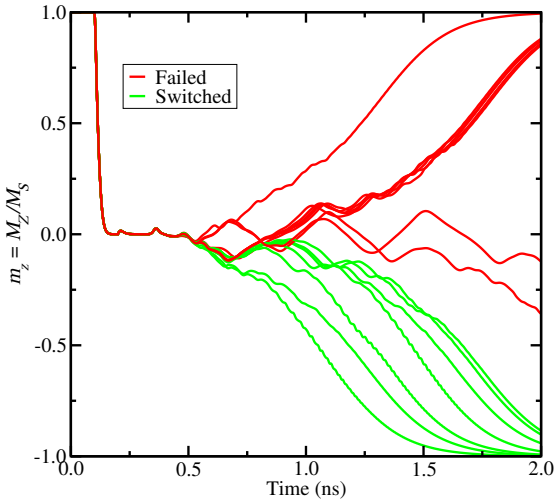

Fig. 4: Magnetization for several realizations for the square device. Deterministic switching is not observed. The switching probability is about 50%.

Fig. 6 demonstrates the typical position dependent magnetization just after the write pulses are applied. As previously explained, after "Pulse 1" is turned on, the magnetization is placed on the plane of the FL along the y direction. Then, due to the SOT of the second pulse the magnetization under the layer NM2 gets rotated towards $-x$ direction, which is shown in Fig. 6. This creates a stray field of the magnetization under the layer NM2, which acts as an effective in-plane magnetic field for the rest of the FL. This field causes the magnetization to precess away from its in-plane orientation towards the switching. Thus, the stray field plays the role of the shape anisotropy field of the rectangular structure.

If we now reduce the width of NM2 for the rectangular device, the switching behavior is that shown in Fig. 7. In this case, besides the existing shape anisotropy field, due to the

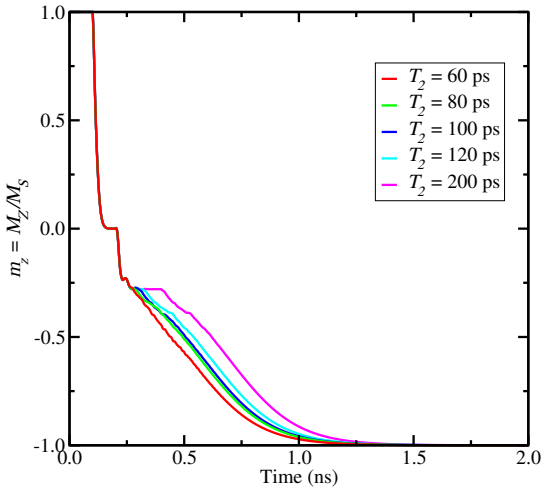

Fig. 5: Average of 20 switching realizations for the square device with $w_2 = 10\,\text{nm}$. Reliable switching is observed for all T_2.

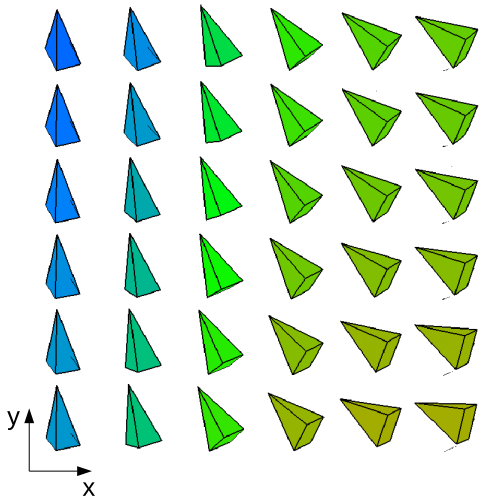

Fig. 6: Snapshot of magnetization for $w_2 = 10\,\text{nm}$ just after "Pulse 2" is on.

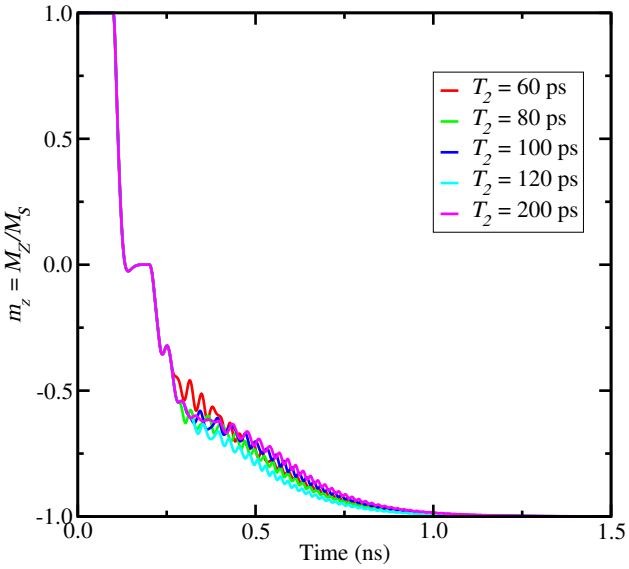

Fig. 7: Average of 20 switching realizations for the rectangular device with $w_2 = 10\,\text{nm}$. Fast and reliable switching is observed for all T_2.

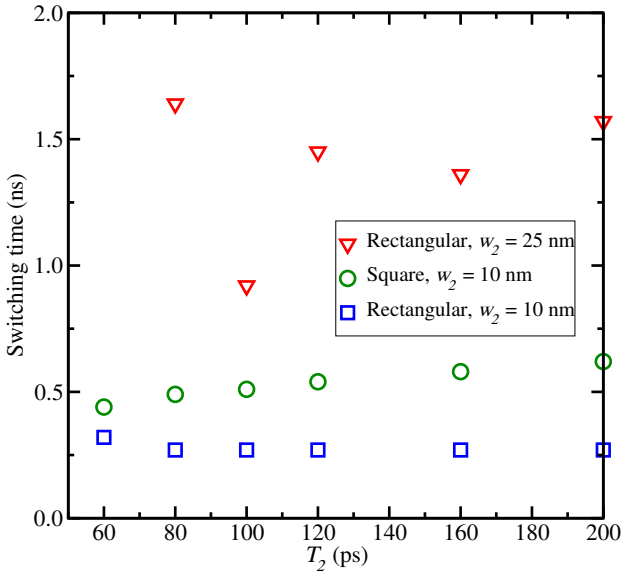

Fig. 8: Switching time as function of T_2 for the different structures. The symbols represent the average of 20 realizations. The error is about the size of the symbol.

reduction of w_2 the effective field has also the contribution of the stray field in part of the structure. The switching time is not only shorter, but also its variation with the second pulse duration T_2 is reduced. Note that the curves nearly coincide. Here, the switching time is about 0.3 ns, remaining practically the same for all cases. A summary of the switching times for the different structures is shown in Fig. 8, where the improvement of the times of the rectangular structure is clearly visible, when the additional stray field is present. It should be noted that this result is accomplished using a smaller current for the second pulse, since the reduction of w_2 implies a decrease of the current magnitude, provided that the current density remains constant.

IV. Conclusion

By using the combination of the shape anisotropy with the stray field the switching of the non-symmetric rectangular structure was accelerated by a factor up to 5 for a smaller current pulse magnitude. A very fast switching time, down to 0.3 ns, was demonstrated. The in-plane stray field created in a part of the free layer remarkably improved the switching of the symmetric square device, turning it into a reliable and fast switching structure. Furthermore, a beneficial influence on the variation of the switching time has been observed. The switching time remains essentially the same for a wide range of pulse durations, thus, it is less sensitive to the input pulse parameters.

Acknowledgment

The financial support by the Austrian Federal Ministry for Digital and Economic Affairs and the National Foundation for Research, Technology and Development is gratefully acknowledged.

References

[1] D. Apalkov, B. Dieny, and J. Slaughter, "Magnetoresistive Random Access Memory," *Proc. of the IEEE*, vol. 104, pp. 1796–1830, 2016.

[2] O. Golonzka, J.-G. Alzate, U. Arslan, M. Bohr, P. Bai, J. Brockman *et al.*, "MRAM as Embedded Non-Volatile Memory Solution for 22FFL FinFET Technology," in *Proc. of the 2018 IEDM*, pp. 18.1.1–18.1.4, 2018.

[3] G. Jan, L. Thomas, and S. Le, "Achieving Sub-ns Switching of STT-MRAM for Future Embedded LLC Applications through Improvement of Nucleation and Propagation Switching Mechanisms," in *Proc. of the 2016 Symp. VLSI Technology and Circuits*, pp. 1–2, 2016.

[4] S.-W. Lee and K.-J. Lee, "Emerging Three-Terminal Magnetic Memory Devices," *Proc. of the IEEE*, vol. 104, pp. 1831–1843, 2016.

[5] I. M. Miron, K. Garello, G. Gaudin, P.-J. Zermatten, M. V. Costache, S. Auffret *et al.*, "Perpendicular Switching of a Single Ferromagnetic Layer Induced by In-Plane Current Injection," *Nature*, vol. 476, pp. 189–193, 2011.

[6] S.-H. C. Baek, V. P. Amin, Y.-W. Oh, G. Go, S.-J. Lee, G.-H. Lee *et al.*, "Spin Currents and Spin-Orbit Torques in Ferromagnetic Trilayers," *Nature Materials*, vol. 17, pp. 509–513, 2018.

[7] G. Yu, P. Upadhyaya, Y. Fan, J. G. Alzate, W. Jiang, K. L. Wong *et al.*, "Switching of Perpendicular Magnetization by Spin-Orbit Torques in the Absence of External Magnetic Fields," *Nature Nanotechnology*, vol. 9, pp. 548–554, 2014.

[8] A. van den Brink, G. Vermijs, A. Solignac, J. Koo, J. T. Kohlhepp, H. J. M. Swagten *et al.*, "Field-Free Magnetization Reversal by Spin-Hall Effect and Exchange Bias," *Nature Communications*, vol. 7, p. 10854, 2016.

[9] Y.-C. Lau, D. Betto, K. Rode, J. M. D. Coey, and P. Stamenov, "Spin-Orbit Torque Switching without an External Field using Interlayer Exchange Coupling," *Nature Nanotechnology*, vol. 11, pp. 758–762, 2016.

[10] J. Yoon, S.-W. Lee, J. H. Kwon, J. M. Lee, J. Son, X. Qiu *et al.*, "Anomalous Spin-Orbit Torque Switching due to Field-Like Torque-Assisted Domain Wall Reflection," *Science Advances*, vol. 3, pp. 1–6, 2017.

[11] V. Sverdlov, A. Makarov, and S. Selberherr, "Reliable Sub-Nanosecond Switching of a Perpendicular SOT-MRAM Cell without External Magnetic Field," *Journal on Systemics, Cybernetics and Informatics*, vol. 16, pp. 55–59, 2018.

[12] (2016) ViennaMag. www.iue.tuwien.ac.at/index.php?id=24.